Design Optimization of Field Emission From A Stacked Carbon Nanotube Array

D. Roy Mahapatra*, N. Sinha**, S.V. Anand***, R. Krishnan***, Vikram N.V.***, R.V.N. Melnik**** and J.T.W. Yeow**

* Department of Aerospace Engineering, Indian Institute of Science, Bangalore, India
** Department of Systems Design Engineering, University of Waterloo,Waterloo, ON, Canada
*** Department of Mechanical Engineering, R.V. College of Engineering, Bangalore, India
**** M^{2}NeT Lab,Wilfrid Laurier University, Waterloo, ON, Canada

ABSTRACT

Fluctuation of field emission in carbon nanotubes (CNTs) is not desirable in many applications and the design of biomedical x-ray devices is one of them. In these applications, it is of great importance to have precise control of electron beams over multiple spatio-temporal scales. In this paper, a new design is proposed in order to optimize the field emission performance of CNT arrays. A diode configuration is used for analysis, where arrays of CNTs act as cathode. The results indicate that the linear height distribution of CNTs, as proposed in this study, shows more stable performance than the conventionally used unifrom distribution.

Keywords: carbon nanotube, field emission, biomedical x-ray devices, electron-phonon, array, electro-mechanical fatigue, optimization.

1 INTRODUCTION

The quest for building functional devices has led to the development of new fabrication techniques and materials, which have been scaled to nano level. The extensive research on nanomaterials can be traced back to the discovery of carbon nanotubes (CNTs) by Iijima in 1991 [1]. Since then newly proposed applications of CNTs such as field emitters, chemical and biological sensors have been successfully demonstrated. With significant improvement in synthesis techniques, CNTs are currently ranked among the best field emitters. CNTs grown on substrates are used as electron sources in field emission applications. Field emission from CNTs is difficult to characterize using simple formulae or data fitting, which is due to (1) electron-phonon interaction; (2) electromechanical force field leading to stretching of CNTs; and (3) ballistic transport induced thermal spikes, coupled with high dynamic stress, leading to degradation of emission performance at the device scale. Fairly detailed physics-based models of CNTs considering the aspects (1) and (2) above have already been developed by the authors [2]-[5]. However, design optimization issues aimed at better field emission devices to reduce the extent of electro-mechanical fatigues and to improve spatio-temporal localization of emitted electrons remain open and important areas of research. With due success in designing such devices, various applications such as in-situ biomedical x-rays probes and thin film pixel based imaging technology, to name just a few, are of great significance. The authors' interest towards this study stems from the problem of precision biomedical x-ray generation. In this paper, we focus on the device-level performance of CNTs grown on a metallic surface in the form of an array (for field emission) under diode configuration. We analyze a new design concept, wherein (a) the electrodynamic force field leading to strong electron-phonon interaction during ballistic transport and also (b) the usually observed reorientation of the CNT tips and instability due to coulomb repulsions, can be harnessed optimally.

2 MODEL FORMULATION

Let N_T be the total number of carbon atoms (in CNTs and in cluster form) in a representative volume element ($V_{\text{cell}} = \Delta A d$), where ΔA is the cell surface interfacing the anode and d is distance between the inner surfaces of cathode substrate and the anode. Let N be the number of CNTs in the cell, and N_{CNT} be the total number of carbon atoms present in the CNTs. We assume that during field emission some CNTs are decomposed and form clusters. Such degradation and fragmentation of CNTs can be treated as the reverse process of CVD or a similar growth process used for producing the CNTs on a substrate. Hence,

$$N_T = N N_{CNT} + N_{\text{cluster}} \,, \tag{1}$$

where N_{cluster} is the total number of carbon atoms in the clusters in a cell at time t and is given by

$$N_{\text{cluster}} = V_{\text{cell}} \int_0^t dn_1(t) \,, \tag{2}$$

where n_1 is the concentration of carbon clusters in the cell. By combining Eqs. (1) and (2), one has

$$N = \frac{1}{N_{CNT}} \left[N_T - V_{\text{cell}} \int_0^t dn_1(t) \right] . \tag{3}$$

The number of carbon atoms in a CNT is proportional to its length. Let the length of a CNT be a function of time, denoted as $L(t)$. Therefore, one can write

$$N_{CNT} = N_{\text{ring}} L(t) \,. \tag{4}$$

where $N_{\rm ring}$ is the number of carbon atoms per unit length of a CNT and can be determined from the geometry of the hexagonal arrangement of carbon atoms in the CNT. By combining Eqs. (3) and (4), one can write

$$N = \frac{1}{N_{\rm ring} L(t)} \left[N_T - V_{\rm cell} \int_0^t dn_1(t) \right] . \qquad (5)$$

In order to determine $n_1(t)$ phenomenologically, we employ a nucleation coupled model developed by us previously [2]. Based on the model, the rate of degradation of CNTs ($v_{\rm burn}$) is defined as

$$v_{\rm burn} = V_{\rm cell} \frac{dn_1(t)}{dt} \left[\frac{s(s-a_1)(s-a_2)(s-a_3)}{n^2 a_1^2 + m^2 a_2^2 + nm(a_1^2 + a_2^2 - a_3^2)} \right]^{1/2} , \qquad (6)$$

where a_1, a_2, a_3 are lattice constants, $s = \frac{1}{2}(a_1+a_2+a_3)$, n and m are integers ($n \geq |m| \geq 0$). The pair (n, m) defines the chirality of the CNT. Therefore, at a given time, the length of a CNT can be expressed as $h(t) = h_0 - v_{\rm burn} t$, where h_0 is the initial average height of the CNTs and d is the distance between the cathode substrate and the anode.

In the absence of electronic transport within a CNT and field emission from its tip, the background electric field is simply $E_0 = -V_0/d$, where $V_0 = V_d - V_s$ is the applied bias voltage, V_s is the constant source potential on the substrate side, V_d is the drain potential on the anode side and d, as before, is the clearance between the electrodes. The total electrostatic energy consists of a linear drop due to the uniform background electric field and the potential energy due to the charges on the CNTs. Therefore, the total electrostatic energy can be expressed as

$$\mathcal{V}(x,z) = -eV_s - e(V_d - V_s)\frac{z}{d} + \sum_j G(i,j)(\hat{n}_j - n) , \quad (7)$$

where e is the positive electronic charge, $G(i,j)$ is the Green's function [6] with i indicating the ring position and $\hat{n}_j$ describing the electron density at node position j on the ring. In the present case, while computing the Green's function, we also consider the nodal charges of the neighboring CNTs. This essentially introduces non-local contributions due to the CNT distribution in the film. We compute the total electric field $\mathbf{E}(z) = -\nabla\mathcal{V}(z)/e$, which is expressed as

$$E_z = -\frac{1}{e}\frac{d\mathcal{V}(z)}{dz} . \qquad (8)$$

The current density (J) due to field emission is obtained by using the Fowler-Nordheim (FN) equation [7]

$$J = \frac{BE_z^2}{\Phi} \exp\left[-\frac{C\Phi^{3/2}}{E_z} \right] , \qquad (9)$$

where Φ is the work function of the CNT, and B and C are constants. Computation is performed at every time step, followed by update of the geometry of the CNTs. As a result, the charge distribution among the CNTs also changes and such a change affects Eq. (7). The field emission current ($I_{\rm cell}$) from the anode surface corresponding to an elemental volume $V_{\rm cell}$ of the film is then obtained as

$$I_{\rm cell} = A_{\rm cell} \sum_{j=1}^{N} J_j , \qquad (10)$$

where $A_{\rm cell}$ is the anode surface area and N is the number of CNTs in the volume element. The total current is obtained by summing the cell-wise current ($I_{\rm cell}$). This formulation takes into account the effect of CNT tip orientations, and one can perform statistical analysis of the device current for randomly distributed and randomly oriented CNTs.

3 RESULTS AND DISCUSSIONS

In the proposed design, we introduce two additional gates on the edges of the cathode substrate. An array of stacked CNTs is considered on the cathode substrate. The height of the CNTs is such that a symmetric force field is maintained in each pixel with respect to the central axis parallel to z-axis (see Fig. 1). As a result, it is expected that a maximum current density and well-shaped beam can be produced under DC voltage across the cathode-anode structure. In the present design, the anode is assumed to be simply a uniform conducting slab. However, such an anode can be replaced with a porous thin film along with MEMS-based beam control mechanism. Figure 1 shows the transverse electric field distribution in the pixel, which directly influences the field emission current.

In the simulation and analysis, the distance between the cathode substrate and anode surface was taken as 34.7 μm. The height of CNTs in arrays was varied between 6 μm to 12 μm. The constants B and C in Eq. (9) were taken as $(1.4 \times 10^{-6}) \times \exp((9.8929) \times \Phi^{-1/2})$ and 6.5×10^7, respectively [8]. It has been reported in the literature (e.g., [8]) that the work function Φ for CNTs is smaller than the work functions for metal, silicon, and graphite. However, there are significant variations in the experimental values of Φ depending on the types of CNTs (i.e., SWNT/MWNT) and geometric parameters. The type of substrate materials have also significant influence on the electronic band-edge potential. The results reported in this paper are based on a representative value of $\Phi = 2.2eV$.

The first step in our computation is to obtain the value of n_1 (the carbon cluster concentration) at a given time step from the nucleation coupled model. In this paper, it has been assumed that at $t = 0$, the diode contains minimal amount of carbon cluster in plasma. The CNTs degrade over time (due to both fragmentation

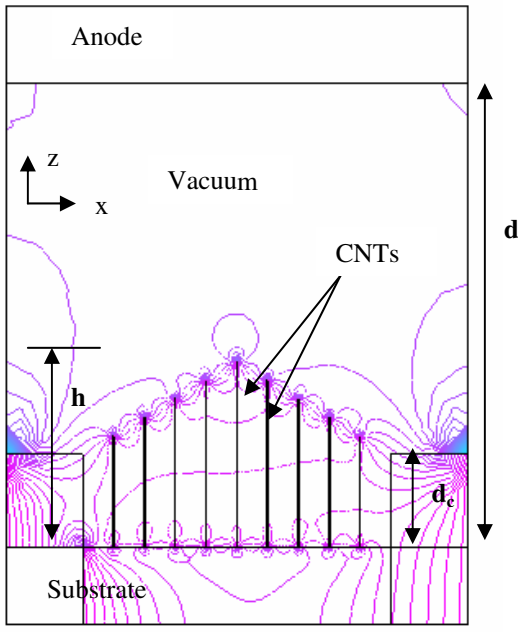

Figure 1: Contour plots of electric field E_z showing the concentration near the CNT tips under symmetric lateral force field. $V_0 = 650$V and the side-wise gates are shorted with the substrate.

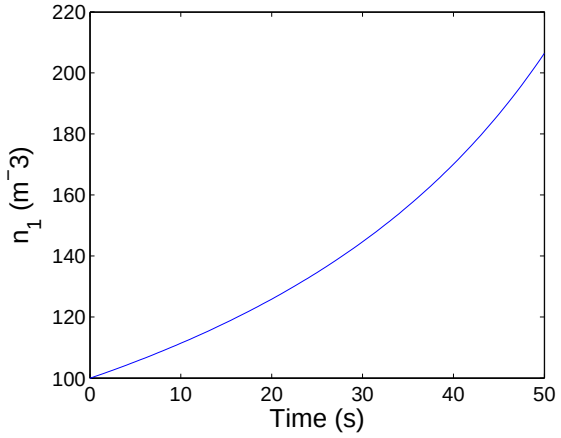

Figure 2: Variation of carbon cluster concentration with time.

and self-assembly) and the carbon cluster concentration in each cell also changes accordingly. Based on this assumption, the value of n_1 was computed. Fig. 2 shows the $n_1(t)$ history over a small time duration ($50s$). Such evolution indicates that the rate of decay is very slow, which in turn implies longer lifetime of cathodes.

Next, we simulate the field emission current histories for two different parametric variations: diameter and spacing between CNTs at the cathode substrate. The current histories are simulated for a constant bias

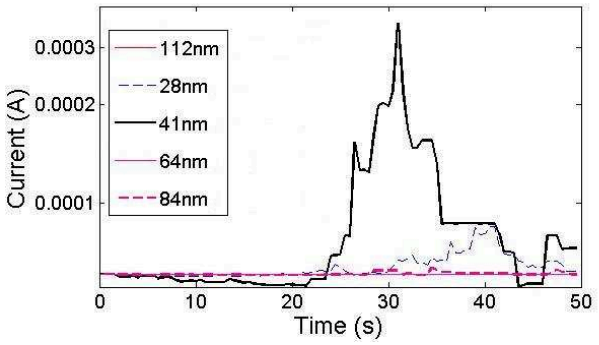

Figure 3: Simulated field emission current histories for varying diameters of CNTs under a DC voltage of 650 V.

voltage of 650 V. In the first case, the spacing between neighboring CNTs is kept constant, while the diameter is varied. The current histories for different values of diameters are shown in Fig. 3. As evident from the figure, the output current is low at large diameter values. This is due to the fact that current amplification is less with large diameter of CNTs.

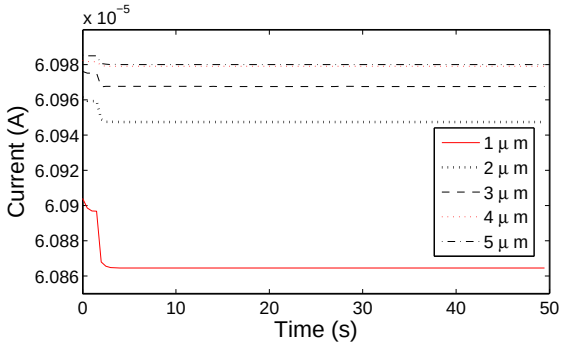

Figure 4: Simulated field emission current histories for varying spacing between neighboring CNTs under a DC voltage of 650 V.

In the second case, the diameter is kept constant, while the spacing between neighboring CNTs is varied. Following five values of spacing between neighboring CNTs have been considered: 1 μm, 2 μm, 3 μm, 4 μm and 5 μm. The current histories for all these cases are shown in Fig. 4. The trends in five curves in Fig. 4 tell us the following: (1) the current in all cases decreases initially and then becomes constant afterwards. This may be due to realignment of CNTs in the array when voltage is applied; (2) as the spacing between neighboring CNTs increases, the output current increases, which is physically consistent because the screening effect becomes less pronounced. These results are in agreement with a previously reported study [9].

Next, we simulate the current-voltage (I-V) charac-

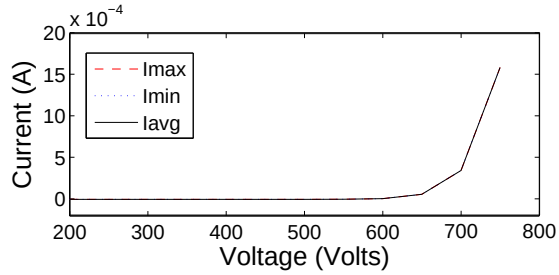

Figure 5: Simulated current-voltage characteristics.

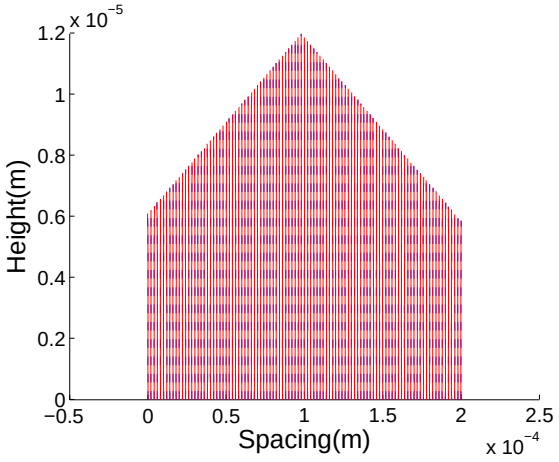

Figure 6: Initial and deflected shape of an array of 100 CNTs at t=50 s of field emission.

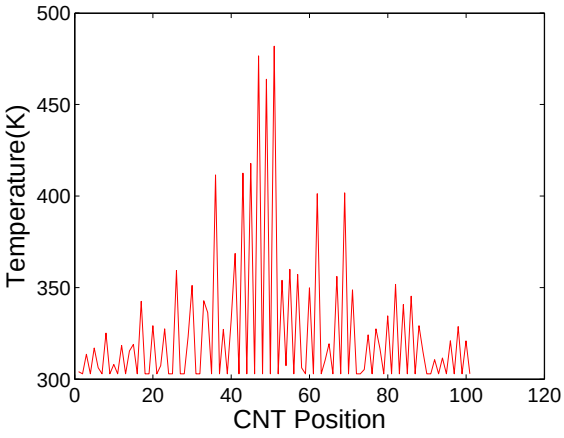

Figure 7: Maximum temperature of CNT tips during 50 s of field emission.

teristics for this arrangement. The minimum, average and maximum values of current were computed. The simulated results are shown in Fig. 5. These results give some interesting insigths. For example, as evident from Fig. 5, the linear height distribution has stabilized the I-V response drastically as compared to uniform height reported in the previous studies. The variation in I-V characteristics for the three cases in this new design is negligible. This is further confirmed by analyzing the simulated results of CNT tip deflections in Fig. 6, in which there is no significant deflection of CNT tips after 50 s.

Finally, in Fig. 7, we plot the maximum tip temperature distribution over an array of 100 CNTs during field emission at a bias voltage of 650 V over 50 s duration. This result indicates a temperature rise of up to $\approx$ 480 K.

4 CONCLUSION

In this paper, a new design concept for the stable performance of CNT arrays in a diode configuration has been proposed. In this design, the CNT height distribution is linearly distributed as opposed to the uniform distribution, considered in most of the previous studies. The results reveal highly stable performance of CNT cathodes in this new design.

REFERENCES

[1] S. Iijima, Nature 354, 56, 1991.

[2] N. Sinha, D. Roy Mahapatra, J.T.W. Yeow, R.V.N. Melnik and D. A. Jaffray, Proc. IEEE Int. Conf. Nanotech., 673, 2006.

[3] N. Sinha, D. Roy Mahapatra, J.T.W. Yeow, R.V.N. Melnik and D.A. Jaffray, J. comp. Theor. Nanosci. 4, 535, 2007.

[4] N. Sinha, D. Roy Mahapatra, Y. Sun, J.T.W. Yeow, R.V.N. Melnik and D.A. Jaffray, Nanotechnology 19, 25710, 2008.

[5] N. Sinha, D. Roy Mahapatra, J.T.W. Yeow and R.V.N. Melnik, Proc. IEEE Int. Conf. Nanotech., 961, 2007.

[6] A. Svizhenko, M.P. Anantram and T.R. Govindan, IEEE Trans. Nanotech. 4, 557, 2005.

[7] R.H. Fowler and L. Nordheim, Proc. Royal Soc. London A 119, 173, 1928.

[8] Z.P. Huang, Y. Tu, D.L. Carnahan and Z.F. Ren, "Field emission of carbon nanotubes," Encyclopedia of Nanoscience and Nanotechnology (Ed. H.S. Nalwa) 3, 401-416, 2004.

[9] L. Nilsson, O. Groening, C. Emmeneger, O. Kuettel, E. Schaller, L. Schlapbach, H. Kind, J.M. Bonard and K. Kern, Appl. Phys. Lett. 76, 2071, 2000.